A CASE STUDY OF HYDROCARBON TRANSPORT ALONG ACTIVE FAULTS AND PRODUCTION-RELATED STRESS CHANGES IN THE MONTEREY FORMATION, CALIFORNIA

Sneha K. Chanchani[1], Mark D. Zoback and Colleen Barton[2]

Department of Geophysics
Stanford University
Stanford, CA 94305

Abstract

Recent field studies show that critically stressed faults, that is, faults that are close to frictional failure in the current stress field, serve as conduits for fluid flow. Similarly, geologic field studies of the low permeability siliceous shales in the Monterey Formation, California clearly indicate that faults influence hydrocarbon transport. We report here a study of the Antelope Shale, a low permeability siliceous shale hydrocarbon reservoir in the Buena Vista Hills field in the southern San Joaquin Valley to determine the influence of the stress state on the relative hydraulic conductivity of the fractures and faults present in the subsurface. Because production has both lowered reservoir pressure and the horizontal stresses, it was necessary to "restore" the reservoir stress state to initial conditions in order to identify correctly the most highly productive intervals. This analysis demonstrates that prior to production, faults in the reservoir were active in a transitional reverse/strike-slip faulting stress state, consistent with regional tectonics. Initial production rates in the field were 2000 bopd, principally from intervals where critically stressed faults were encountered.

Introduction

The relationship between the in situ state of stress and the orientation of hydraulically conductive fractures is conventionally viewed in the context of mode I extension fractures oriented perpendicular to the least principal stress (Secor, 1965; du Rouchet, 1981; Nur and Walder, 1990). Such a relationship has straightforward implications for utilizing geophysical techniques such as seismic velocity anisotropy, shear-wave splitting, and amplitude versus offset (AVO) to identify in situ directions of permeability anisotropy in regions where fracture permeability is important (e.g.,

---

[1] Current Address: BP-Amoco Exploration, 501 Westlake Park Boulevard, Houston, TX 77479 USA
[2] Current Address: GeoMechanics International, Inc. 250 Cambridge Ave., Palo Alto, CA 94306 USA

Crampin 1993, Winterstein and Meadows, 1991). In this paper, we investigate an alternative hypothesis in which critically stressed faults, that is faults close to frictional failure in the in situ stress state, may be responsible for hydrocarbon transport in reservoir rocks with low primary permeability.

Barton et al. (1995) demonstrated that in crystalline rock, fractures and faults that were critically-stressed for frictional failure in the current stress field, were also hydraulically conductive. Finkbeiner et al. (1997) documented a similar increase in formation permeability in 4 wells in the Santa Maria basin, California, at depth intervals of brittle lithologies and critically stressed fracture and bedding planes. In a field study of sedimentary rocks, Dholakia et al. (1998) showed the predominant association between faulting, fault-related fractures and the occurrence of petroleum in siliceous shale deposits of the Monterey Formation. Petroleum-staining in surface exposures of the Monterey Formation was observed primarily within fault zones and fault-related fractures. This field study identified fault development in surface exposures of low permeability siliceous shale along the central California coast and in the San Joaquin Valley. As faulting developed, the low permeability rocks systematically fragment and subsequently brecciate to increase permeability locally, and facilitate hydrocarbon transport. These studies support the hypothesis that fluid flow is not simply controlled by mode I extension fractures oriented perpendicular to the minimum horizontal stress, but rather that shear faults are important for hydrocarbon transport.

Efforts to understand fracture controls on hydrocarbon transport and accumulation in tight, low permeability siliceous shales are being pursued as part of a multidisciplinary project to develop enhanced oil recovery methods for further extraction of trapped hydrocarbons within the siliceous shale. As part of this study, we have investigated the Buena Vista Hills field to determine the potential for hydrocarbon production from fracture permeability and the influence of reservoir depletion on the current stress field.

The Buena Vista Hills field, discovered in 1952, is located in the southern San Joaquin Valley, approximately 40 km (25 miles) southwest of Bakersfield, California (Figure 1). The field was drilled initially in the 1950's and 1960's, and is situated on a NW-SE doubly-plunging anticline paralleling the San Andreas Fault. Initial production rates from individual wells peaked at 2000 bopd with daily production rates dropping to 6 bopd in the 1970's. Recent well stimulation efforts have brought the rate to 20 bopd. Total production to date from the field is 9 million barrels of oil, only 6.5% of the estimated oil in place in the Antelope Shale in the Buena Vista Hills field. The Antelope Shale pay thickness is about 244 m (800 ft) at a depth ranging from 1189-1524 m (3900-5000 ft). Porosity ranges from 20-40% and matrix permeability is 0.5-1 md. Initial pressure in the reservoir was 13.8 MPa (2000 psi), and has since dropped to 5.5 MPa (800 psi) leading to further

production difficulties (written comm., Chevron, 1994). In a recent paper, Montgomery and Morea (2001) describe the Antelope shale reservoir in some detail.

Stress Orientations and Active Tectonics

Wellbore breakouts, reverse fault earthquake focal mechanisms, and hydraulic fracture orientations along the length of the Coast Ranges in Central California indicate a northeast-southwest direction of maximum horizontal compression (S_{Hmax}) nearly perpendicular to the San Andreas Fault system (Zoback, et al., 1987; Mount and Suppe, 1987; Wentworth and Zoback, 1989). Axes of young, active folds along the Coast Ranges lie nearly perpendicular to the northeast-southwest directed S_{Hmax} suggesting anticlinal development driven by seismogenic blind thrusts is an active process in the current stress field. Figure 2 is a regional stress map showing the S_{Hmax} direction determined from various stress indicators (e.g. wellbore breakouts, earthquake focal mechanisms, and hydraulic fractures) and geologic structures in the San Joaquin Valley. The gray symbols reflect earlier studies on the state of stress in California (Mount and Suppe, 1987; Zoback, et al., 1987; Castillo and Zoback, 1995). The black symbols represent new data collected for this study from tiltmeter measurements of hydraulic fracture tests, which are described in more detail below. The lengths of each stress indicator are weighted according to a quality-ranking scheme (Zoback and Zoback, 1991) based on the standard deviation, depth of observation, and number of observations.

In this study, in situ stress orientations were considered in the area shown by the inset of Fig. 1 using new data from tiltmeter surveys of hydraulic fractures in 56 wells from Belridge, Lost Hills, and Cymric fields by Pinnacle Technologies (written comm., C. Wright) were collected and compiled. Hydraulic fractures propagate in a direction perpendicular to the minimum principal compressive stress in the crust (Hubbert and Willis, 1957). The deformation, or local displacement gradients, at the surface induced by the hydraulic fracture is a function of the fracture orientation. Utilization of tiltmeters for determining the azimuth of large-scale, near-vertical, hydraulic fractures at relatively shallow depth is described by Wright (1998). Because of the high density of data available, the hydraulic fracture orientations were averaged with depth within an individual well and with other wells located within a one mile radius in a given field.

The seven hydraulic fracture orientations indicated in black with the open diamond symbol represent fracture orientations from wells within the Cymric field and the northern, central and southern areas of both Lost Hills and Belridge fields (Figure 2). The average hydraulic fracture orientations were computed for vertical or near vertical fractures, dipping greater than 70° from

horizontal, and occurring below 300 m depth. The statistical mean fracture orientation and standard deviations were computed using the method described by Mardia (1972) for azimuthal data and are shown in Table 1.

Table 1: Summary of S_{Hmax} orientations determined from tiltmeter measurements of deformation caused by hydraulic fractures. Each orientation reflects the average of several fractures wells within a one-mile radius.

Field Name	**S_{Hmax} Direction**	**Number of Hydraulic Fractures**
Cymric	N12.5°E ±3.2°	6
North Belridge	N40.3°E ±3.6°	21
Central Belridge	N15.7°E ±3.7°	15
South Belridge	N20.5°E ±2.9°	59
North Lost Hills	N35.5°E ±1.2°	5
Central Lost Hills	N53.7°E ±4.3°	34
South Lost Hills	N52.7°E ±3.2°	28

Wellbore breakout analyses of FMS data were also conducted within the Buena Vista Hills field. Wellbore breakouts refer to spalled regions of the borehole in which the circumferential stress around the borehole exceeds the compressive strength of the rock. The borehole is elongated in the direction of the minimum horizontal stress (Bell and Gough, 1979; Zoback et al., 1985) and is considered a reliable indicator of horizontal stress directions (e.g. see discussion is Zoback and Zoback, 1991). The orientation of S_{Hmax} determined from the breakout analyses of FMS data of two wells in the Buena Vista Hills field are shown on the stress map in black by the two inward pointed arrows (Figure 2). The breakout information was obtained from the caliper surveys of the FMS log. The azimuthal mean orientation and standard deviation of the breakouts are listed in Table 2 and were computed using the method described by Mardia (1972). Like the tiltmeter surveys of the hydraulic fracture, the points on the map are length-weighted according to data quality. Data quality factors for wellbore breakout data include the number of breakout intervals, the total length of breakouts within the wellbore, the standard deviation, and the depth of observation (Zoback and Zoback, 1991).

Table 2: Summary of S_{Hmax} directions determined from wellbore breakout analysis of two wells in Buena Vista Hills field.

Well Name	S_{Hmax} Direction	Breakout Length
621-25B	N8°E ±6°	65 m
723-9D	N21°E ±7°	229 m

The breakout analyses and tiltmeter surveys indicate a northeast-southwest directed S_{Hmax}, oriented nearly perpendicular to the San Andreas Fault and the axes of young, active folds along the Coast Ranges. This near perpendicular relationship suggests active structural development and deformation in the current stress field (Zoback et al., 1987; Mount and Suppe 1987, 1992; Wentworth and Zoback, 1989).

Constraining Stress Magnitudes

Knowledge of the orientation and magnitude of the in situ stress is required to determine which subsurface fractures and faults are most important for hydrocarbon transport. In this section we first constrain the current horizontal principal stress magnitudes and then attempt to extrapolate back in time to assess the stress state prior to reservoir pressure depletion. In Buena Vista Hills field, we determine the current stress orientation and magnitude to evaluate the influence of the in situ stress state on fractures in the reservoir identified using borehole image data.

Stress Magnitudes in 1989

As supported by tiltmeter data (Castillo et al., 1997; Wright, 1998), we assume that the principal stresses act in three orthogonal directions, one near-vertical, normal to the surface of the earth, and in two orthogonal horizontal directions (S_{hmin} and S_{Hmax}). The vertical stress (S_v) is assumed to be equal to the weight of the overlying rock. Density logs were integrated with depth to determine S_v. The overlying lithologies consist primarily of low density diatomite and siliceous shale, and the densities reported in the density log are consistent with laboratory measurements of siliceous rocks (2.0-2.3 g/cm^3) (Isaacs, 1981).

Hydraulic fracturing of the wells to enhance production provides direct measures of the minimum principal stress magnitude. The fluid pressure required to propagate a hydraulic fracture is a measure of the minimum horizontal stress magnitude (S_{hmin}) when $S_{hmin} \leq S_v$ (Hubbert and Willis, 1957; Kehle, 1964; Haimson and Fairhurst,1970). S_{hmin} values corresponding to three hydraulic fracturing tests at different depths conducted in 1989 are provided in Table 3.

Table 3: Summary of S_{hmin} with depth determined from hydraulic fracture tests. The average S_{hmin} is used in this study.

Depth (m)	S_{hmin} (MPa)
1204	18
1289	20
1341	22
	Average S_{hmin} = 20

In Buena Vista Hills field we constrain the magnitude of the maximum compressive stress (S_{Hmax}) by employing simple elastic failure criterion and wellbore failure analysis following Moos and Zoback (1990). Breakouts in this study were detected using 4-arm dipmeter data and analyzed in accordance with criteria proposed by Plumb and Hickman (1985). A wellbore breakout will form when the stress concentration around the wellbore exceeds the compressive strength of the rock, C_o (Zoback et al. 1985, Moos and Zoback 1990) and is described by the following equation:

$$S_{Hmax} + S_{hmin} - 2(S_{Hmax} - S_{hmin})\cos 2\theta - 2P_o \geq C_o \quad (1)$$

Consideration of the breakout's width ($2\theta_B$) can be used to better constraint S_{Hmax} as for a given rock strength, S_{Hmax} must be sufficiently high to have caused the breakout to have a given width (Barton et al., 1986). In order for breakouts to be detected in the FMS data, the breakout must be at least as wide as the FMS pad or the pad would not have fallen into the breakout. We assume that the minimum breakout width is ≥54°, the width of the FMS pad, and is centered at the azimuth of S_{hmin}. Equation 1 leads to the following:

$$2.18S_{Hmax} - 0.18S_{hmin} - 2P_o \geq C_o \quad (2)$$

which leads to

$$S_{Hmax} \geq .46(C + 0{,}18S_{hmin} + 2P_o) \quad (3)$$

where P_0 is the pore pressure in the formation at the time the well is drilled and the mud weight is essentially equal to the pore pressure.

Uniaxial compressive rock strength values, C_o, for the Antelope Shale were measured directly in triaxial compression tests at the depths listed in Table 3. Rock strength values were found to be quite high and range from 92 - 126 MPa (written comm., Chevron 1994). The shear modulus computed from the shear wave and compressional wave velocities determined from the sonic log at

the depth from which the laboratory samples were tested are much higher (4.2-4.9 GPa) than the values from the intervals at which breakouts occur (3.4 GPa). This difference in shear moduli suggests that the compressive rock strength values used to constrain S_{Hmax} is likely to be lower than the average laboratory measured value of 110 MPa. Compressive rock strength tests on siliceous sediments from an offshore well in the Monterey Formation yield much lower values between 25 MPa and 117 MPa (C. Bovberg, personal communication). Thus, there is considerable uncertainty in the appropriate rock strength in this formation. Using a compressive rock strength value of 90 MPa establishes a lower bound for S_{Hmax} of about 48 MPa.

Considering the state of stress in the earth's crust to be limited by its frictional strength, the allowable stress states are given by

$$\frac{S_1 - P_o}{S_3 - P_o} \leq \left[\left(1 + \mu^2\right)^{\frac{1}{2}} + \mu\right]^2 \qquad (4)$$

where P_O is the pore pressure and μ is the coefficient of sliding friction (e.g., Jaeger and Cook, 1979). Frictional equilibrium of the earth's crust where $\mu = 0.6$ suggests an upper limit of S_{Hmax} of 50 MPa. Thus, in 1989, the average state of stress appears to be a strike-slip regime in which the stresses are as follows:

$$S_{hmin} = 20 \text{ MPa}$$
$$S_v = 25 \text{ MPa}$$
$$48 \text{ MPa} \leq S_{Hmax} \leq 50 \text{ MPa}$$

Stress Magnitudes in 1952

Drilling in the Buena Vista Hills field in the Antelope Shale began in 1952 and continued to 1989. Reservoir depletion and drilling through time lowered the pore pressure and thus, lowered the horizontal stresses poroelastically. During this time the reservoir pressure has declined significantly from 13.8 MPa (2000 psi) in 1952 to approximately 5.5 MPa (800 psi) in 1989 (Figure 3). From the hydraulic fracture tests in 1989, we know the average S_{hmin} is 20 MPa (Table 3). Because of the large pressure decline in the reservoir, the state of stress in 1989 reflects lower magnitudes of stress than that which existed prior to reservoir depletion.

The magnitude of S_{hmin} measured in 1989 reflects the minimum horizontal stress at the time of hydraulic fracture testing and not the stress state in the undisturbed reservoir. In order to extrapolate the minimum horizontal stress to initial conditions in the Antelope Shale, $S_{hmin1952}$, we

employ the theory of poroelasticity which describes the change in the horizontal stresses as a function of pore pressure, P_O (Biot, 1941; Segall, 1992). Approximating the reservoir shape as flat and infinite in lateral extent, the change in the horizontal stresses as a function of the change in P_O may be expressed as follows:

$$\Delta Sh = \Delta P_o \alpha \frac{1 - 2\nu}{1 - \nu} \quad (5)$$

where α is the Biot coefficient of effective stress and ν is the undrained Poisson's ratio (Segall, 1992). The Biot coefficient of effective stress, α, is defined as follows:

$$\alpha = \left(1 - \frac{k_b}{k_g}\right)$$

where k_b is bulk modulus of the dry porous frame and k_g is the bulk modulus of the grains. When k_b is small, and α approaches 1, the largest fluid effects are observed. A high porosity, soft sediment rock similar to the siliceous shale of the Monterey Formation will have $\alpha \sim 1$ (e.g. Krief et al., 1990; Segall et al., 1994). We use $\alpha \sim 1$, and from laboratory triaxial compression tests, ν is approximately 0.23 (Table 4). Substituting these values in equation 4, the ratio of the change in horizontal stress to pore pressure in the reservoir is $\Delta Sh/\Delta Po \sim 0.70$, similar to values reported by Engelder and Fischer (1994) in other areas. Figure 3 illustrates the decline in the horizontal stresses through time as a function of reservoir depletion. The horizontal stresses decreased by about 5.8 MPa. Note that while the state of stress in 1989 appears to be a strike-slip stress state ($S_{Hmax} > S_V > S_{hmin}$), the original stress state in the reservoir appears to have been a reverse faulting regime ($S_{Hmax} > S_{hmin} > S_V$). Because S_{hmin} is only slightly greater than S_V, it is indicative of a transitional reverse/strike-slip faulting regime. Thus, in 1952, the state of stress appears to be as follows:

$$S_V = 25 \text{ MPa}$$
$$S_{hmin} = 26 \text{ MPa}$$
$$S_{Hmax} \geq 54 \text{ MPa}$$

Table 4: Compressive rock strengths measured in triaxial compression.

Sample Depth (m)	**Poisson's Ratio, ν**	**Strength, C (MPa)**
1172	0.23	92
1306	0.22	113
1395	0.25	126

Fractures, Faults and Production

Microresistivity borehole image, FMS, data from the Buena Vista Hills field provides an opportunity to identify fractures and fracture zones and to determine the effect of the stress state prior to reservoir production in 1952 on fluid flow. The FMS tool consists of 4 pads, 2 orthogonal pads with microresistivity imaging electrodes and 2 pads with standard dipmeter electrodes (Ekstrom et al., 1987). The image data is typically displayed as if the walls of the borehole were unwrapped and laid flat. Fractures intersecting the borehole would thus appear as a sinusoid cutting across the individual image pad displays.

Fractures, bedding, and other zones of disrupted appearance are identified in the FMS images from the Chevron well 621-25B. Only a partial section of approximately 343 m (1,125 ft) of the Antelope Shale section, below the opal A/opal CT diagenetic contact, was logged. Over 300 fractures were identified in the logged interval of image data of the Antelope Shale. The relative fracture frequency with depth in the 621-25B well (Figure 4) is related to lithology differences. It is known from the core that the Antelope Shale beds dip at a low angle, therefore low angle (<10°), planar features in the image data are interpreted to be bedding. The Antelope shale contains more fractures than the Brown shale. The Brown shale is more clay-rich, whereas the Antelope shale consists of thin graded siliceous shale beds, porcelanite and chert beds. The Antelope shale is more brittle and contains more fractures (written comm., Chevron 1994).

In this study we are concerned with the influence of the present day stress state and the impact of reservoir depletion on production. Measured matrix permeabilities of core plugs from the Antelope Shale are very low, 0.1-0.5 md. The low permeability, tight nature of the Antelope Shale suggests production is primarily from fracture permeability. The stress analysis shows the environment to be in a transitional strike-slip to reverse faulting regime in which the intermediate and minimum, S_2 and S_3, principal stresses are nearly equal. Transitional strike-slip/reverse stress state is consistent

with the stress inversion of the 1952 Kern County M*s* 7.8 earthquake and contemporary seismicity occurring approximately 30 km southwest of Buena Vista Hills field (Castillo and Zoback, 1995).

The poles to the fracture planes identified in the image data and directions of S_{Hmax} determined from the wellbore breakout analysis are plotted in the stereonet in Figure 5. The fractures observed concentrate in two broad regions as conjugate reverse faults. Colors on the stereonet illustrates the normalized Coulomb failure function (CFF) and critical Pp (that required to induce slip) as a function of fracture orientation and poles in white indicated the critically stressed faults (fracture poles falling in the red-shaded region). The Coulomb failure function is defined in the following equation:

$$CFF = \tau - \mu(S_n - P_p) \tag{6}$$

where τ is the shear stress acting on a fault plane, S_n is the normal stress and Pp is the ambient pore pressure. μ is the coefficient of friction and is taken as 0.6. Thus, when CFF $\geq$0.6 faults are critically-stressed and when CFF $\leq$0.6 they are not. The figure indicates that conjugate reverse faults or fractures are more likely to slip in the transitional strike-slip/reverse stress regime. It is clear to see that there are many critically-stressed faults in reservoir.

Comparison of the critically stressed fracture occurrence with production data suggests a qualitative relationship between critically stressed fractures and fluid flow (Figure 4). According to Chevron (1994), the most productive interval in the 621-25B is in the Upper and Lower Antelope Shale between the Pa and P2a markers. The Lower Antelope Shale from P1b to P2a accounts for two-thirds of the fluid produced from the well. Historically, in the Buena Vista Hills field, the P-P1b is the most productive interval. Spinner flowmeter production logging in the perforated intervals in Chevron well 621-25B (Figure 4) shows the distribution of flow rates in the wellbore. Spinner flowmeter tools measure the flow rate (revolutions per second) below the tool, and the black bars in Figure 4 show the relative magnitudes of flow rate as a function of depth. Overall, the productive interval in the Antelope Shale interval contains many critically stressed faults. There are also critically-stressed faults in the Brown shale where the flow meter survey indicated significant flow. However, as the flow meter survey did not cover both formations, it is not clear what the response would have been in the most productive section of the Antelope shale and the respective abundance of critically-stressed faults.

Discussion

The Antelope Shale at Chico Martinez Creek (Dholakia et al., 1998) serves as a surface analog to the subsurface reservoir at Buena Vista Hills field. Not only are both areas structurally similar anticlines associated with the San Andreas fault, but also the section studied at Chico Martinez Creek correlates to portions of the producing reservoir in the BVH field. The Chico Martinez Creek outcrop, 56 km northwest of BVH, exposes the Antelope Shale Member of the Monterey Formation, the reservoir unit at BVH, in the northeastern limb of the anticline. In addition, the diagenetic grade of the Antelope Shale at both localities consists of siliceous shale and porcelanite. The Antelope Shale outcrop study by Dholakia et al. (1998) at Chico Martinez Creek in the San Joaquin Valley documents a predominant association between hydrocarbon transport and brecciated fault zones. Petroleum staining occurs in bed-parallel breccia zones. Observations of hydrocarbon-stained breccia and rubble zones in core from Buena Vista Hills and neighboring fields, along with evidence from surface exposures, directly support the relationship between shearing deformation and hydrocarbon flow pathways and storage in the subsurface. Figure 6 (modified from Dholakia et al., 1998) shows an oil-saturated breccia zone in core from a well in the Antelope shale in the Cymric field as well as a diagrammatic illustration of the way in which shear deformation induces brecciation and enhanced permeability.

A major shortcoming of this work is our inability to compare, in detail, the affect of individual, or sets, of critically-stressed faults on productivity. This would also make it possible to further investigate other factors such as lithology, fault orientation, apparent aperture, etc.

Conclusions

This case study of the Antelope shale, Monterey Formation, demonstrates that faults active in the current stress state correlate with intervals of higher productivity. Stress analysis indicates that prior to production, faults in the reservoir were active in a transitional reverse/strike-slip faulting regime, consistent with regional tectonics. Because production has both lowered reservoir pressure and the horizontal stresses, the initial reservoir stress state was "restored" to identify correctly the most highly productive intervals. Comparison of the critically stressed fracture occurrence with production data suggests a qualitative relationship between critically stressed fractures and fluid flow. This subsurface geophysical study at Buena Vista Hills field supports the hypothesis that fractures close to frictional failure, *active faults,* are important for hydrocarbon transport.

Acknowledgements

This work was supported by Chevron USA, the Department of Energy contract DE-PS22-94BC1114973, the Stanford Borehole Geophysics Laboratory, the Stanford Rock Fracture Project and the Phillips Fellowship. We thank Chris Wright of Pinnacle Technologies for additional stress data in the San Joaquin basin from tiltmeter surveys of hydraulic fracture tests. We thank Bruce Bilodeau of Chevron Production Co. for subsurface data and discussion critical for this study

References

Barton, C. A., Zoback, M. D. and Burns K. L., 1988, In situ stress orientation and magnitude at the Fenton Geothermal site, New Mexico, determined from wellbore breakouts. Geophys. Res. Let., **15**, 467-470.

Barton, C. A., Zoback, M. D., and Moos, D., 1995, Fluid flow along potentially active faults in crystalline rock. Geology, **23**, 683-686.

Bell, J. S., and Gough, D. I., 1979, Northeast-southwest compressive stress in Alberta: evidence from oil wells. Earth and Planet. Sci. Lett. **45**, 475-482.

Biot, M. A., 1941, General theory of three-dimensional consolidation: J. of Appl. Phy., **12**, p. 155-164.

Castillo, D. A. et al., 1997, Deep Hydraulic fracture imaging: Recent advances in tiltmeter technologies. International Journ. Of Rock Mechanics & Mining Services, **34**.

Castillo, D. A. and Zoback, M.D., 1995, Systematic stress variations in the southern San Joaquin Valley and along the White Wolf fault: Implications for the rupture mechanics of the 1952 Ms 7.8 Kern County earthquake and contemporary seismicity: J. of Geophys. Res., **100**, 6249-6264.

Chevron Production Company, 1994, U. S. Dept. of Energy Technical Proposal: Advanced Reservoir Characterization in the Antelope Shale to establish viability of CO2 enhanced oil recovery in California's Monterey siliceous shales. vol. IIA.

Crampin, S., 1993, A review of the effects of crack geometry on wave propagation through aligned cracks, Canadian Journal of Exploration Geophysics, **29**, 3-17.

Dholakia, S. K., Aydin, A., Pollard, D. D., and Zoback, M. D., 1998, Fault-controlled hydrocarbon pathways in the Monterey Formation, California, AAPG Bull., **82**, 1551-1574.

Du Rouchet, J., 1981, Stress fields, a key to oil migration, AAPG Bull., **65**, 74-85

Ekstrom, M.P. et al., 1987, Formation Imaging with microelectrical scanning arrays: The Log Analyst, 294-306.

Engelder, T. and M. P. Fischer, 1994, Influence of poroelastic behavior on the magnitude of minimum horizontal stress, S_h, in overpressured parts of sedimentary basins, Geology, **22**, 949-952.

Finkbeiner, T., Barton, C. A., and Zoback, M. D., 1997, Relationship among in-situ stress, fractures and faults, and fluid flow: Monterey Formation, Santa Maria Basin, California, AAPG Bull., **12**, 1975-1999.

Graham, S. A., and L. A. Williams, 1983, The Monterey Formation tapped for big pays: AAPG Explorer, **5**, 1-5.

Haimson, B. and Fairhurst, C., 1970, In situ stress determination at great depth by means of hydraulic fracturing, Ch 28. In Rock Mechanics—Theory and Practice, Soc. Mining Eng., 559-584.

Hubbert, M. K. and Willis, D. G., 1957, Mechanics of hydraulic fracturing, AIME Petroleum Transactions, **210**, 153-166.

Isaacs, C. M., 1981, Porosity reduction during diagenesis of the Monterey Formation, Santa Barbara coastal area, California. *in* C. M. Isaacs and R. E. Garrison, eds. Petroleum Generation and Occurrence in the Miocene Monterey Formation, California: Pacific Section SEPM, 257-271.

Jaeger, J. C. and Cook, N.G.W., 1979, Fundamental of rock mechanics, 2nd ed., Methuen and Co., London, 315 p.

Kehle, R. O., 1964, The determination of tectonic stresses through analysis of hydraulic well fracturing. J. Geophys. Res., **69**, 259-273.

Krief, M., Garat, J., Stellingwerff, J., and Ventre, J., 1990, A petrophysical interpretation using the velocities of P and S waves (full-waveform sonic): The Log Analyst, 355-369.

Liu, E., Crampin, S., Queen, J. H., Rizer, W. D., 1993, Behaviour of shear waves in rocks with two sets of parallel cracks. Geophys. J. Int., **113**, 509-517.

Mardia, R. V., 1972, Statistics of directional data: London and New York, Academic Press, 357 p.

Moos, D. and Zoback, M.D., 1990, Utilization of wellbore failure to constrain the orientation and magnitude of crustal stresses: Application to Continental, Deep Sea Drilling Project, and Ocean Drilling Program boreholes. J. Geophys. Res., **95**, 9305-9325.

Montgomery, S.L. and M.F. Morea, 2001, Antelope shale (Moneterey Formation), Buena Vista Hills field: Advanced reservoir characterization to evaluate CO2 injection for enhanced oil recovery, Amer. Assoc. Petrol. Geol., **85**, 56-585.

Mount, V. S. and Suppe, J., 1987, State of stress near the San Andreas fault: implications for wrench tectonics, Geology, **15**, 11143-1146.

Mount, V. S. and Suppe, J., 1992, Present-day stress orientations adjacent to active strike-slip faults: California and Sumatra, J. of Geophys. Res., **97**, 11955-12013.

Nur, A. and Walder, J., 1990, Time-dependent hydraulics of the earth's crust. *in* The role of fluids in crustal processes. Geophysics Study Committee, National Academy of Sciences.

Plumb, R. A. and Hickman, S. H., 1985, Stress-induced borehole elongation: A comparison between the four-arm dipmeter and the borehole televiewer in the Auburn geothermal well. J. of Geophys. Res., **90**, 5513-5521.

Secor, D. T., 1965, Role of fluid pressure in jointing, Am. J. Sci., **263**, 633-646.

Segall, P., 1992, Induced stresses due to fluid extraction form axisymmetric reservoirs: Pure and Appl. Geophys. **139**, 535-560.

Segall, P., Grasso, J. R., and Mossop, A., 1994, Poroelastic stressing and induced seismicity near the Lacq gas field, southwestern France: J. of Geophys. Res., **99**, p. 15,423-15,438.

Wentworth, C. M. and Zoback, M. D., 1989, The style of Late Cenozoic deformation at the eastern front of the California Coast Ranges, Tectonics, **8**, 237-246.

Winterstein, D. F. and Meadows, M. A., 1991, Shear-wave polarizations and subsurface stress directions at Lost Hills field. Geophysics, **56**, 1331-1348.

Wright, C., 1998, Tiltmeter fracture mapping: from surface and now downhole. Petroleum Engineer International, **71**, 50-63.

Zoback, M. D., Moos, D., Mastin, L., and Anderson, R. N., 1985, Wellbore breakouts and in situ stress. J. of Geophys. Res. **90**, 5523-5530.

Zoback, M. D., et al., 1987, New evidence on the state of stress of the San Andreas fault system. Science, **238**, 1105-1111.

Zoback, M. D. and Zoback, M. L., 1991, Tectonic stress field of North America and relative plate motions, *in* Siemmons, D. B., Engdahl, E. R., Zoback, M.D., and Blackwell, D. D., eds., Neotectonics of North America: Boulder, Colorado, Geol. Soc. of Am., Decade Map Volume.

Figure Captions

Figure 1: (A) Location of major Neogene basins in California (from Graham and Williams, 1983). (B) Location of the Buena Vista Hills field and other major oil fields in the southern San Joaquin basin.

Figure 2: Regional stress map in southern San Joaquin and Santa Maria basins, California. The symbols in black represent new data collected for this study from tiltmeter measurements of hydraulic fracture tests.

Figure 3: General pressure decline curve for the Buena Vista Hills field that illustrates the change in horizontal stresses and pore pressure through time.

Figure 4: Tadpole plot of the fracture frequency and orientation with depth. The red tadpoles are the ones that are critically stressed. The green ones are mode I cracks, normal to the least principal stress. These are plotted in white in Fig. 5.

Figure 5: The stereonet illustrates the degree to which fractures and faults are critically stressed as the excess pore pressure required to cause fault. Critically-stressed fractures are highlighted in white (require no excess pore pressure to be active) and correspond to the red tadpoles in Fig. 4. The critically-stressed fractures observed in the 621-25B well concentrate in two broad regions as conjugate reverse/strike-slip faults.

Figure 6: Photograph of oil-stained breccia zone in Antelope shale core from the Buena Cymric field and a schematic diagram illustrating the way in which progressive shear deformation leads to development of breccia zones and enhanced permeability (modified after Dholakia et al., 1998).

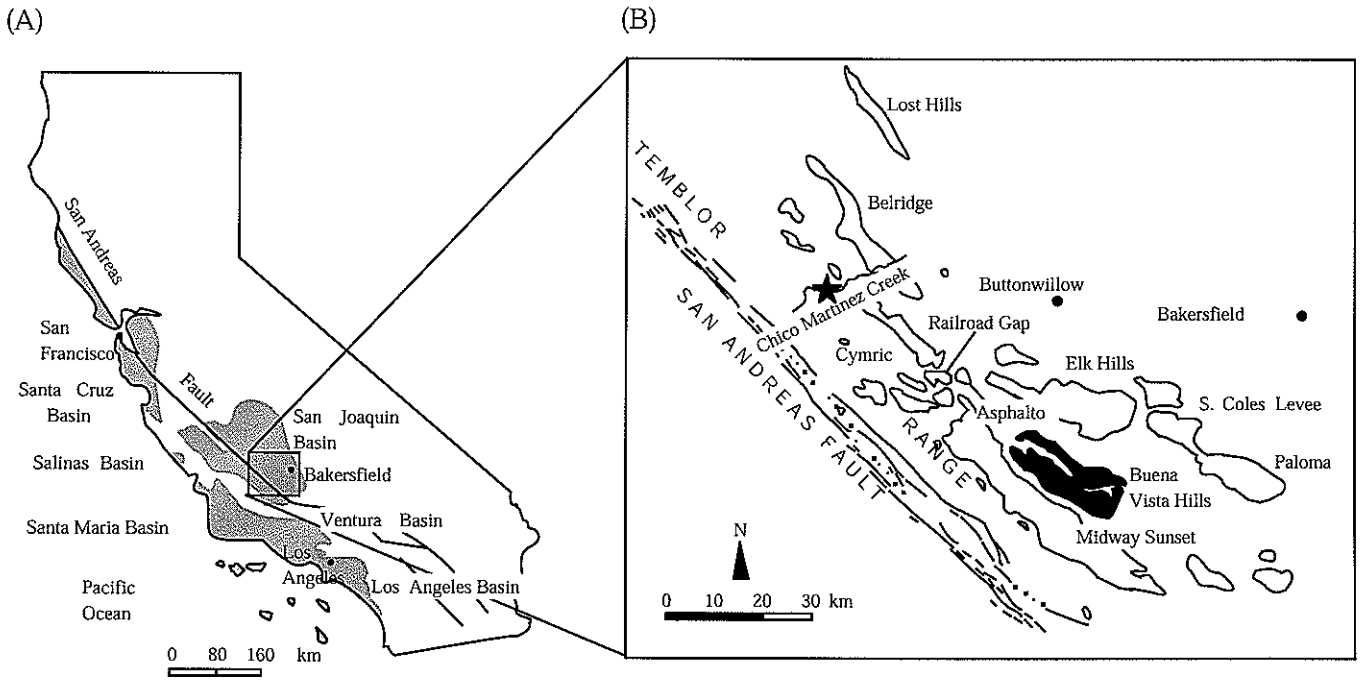
(A)
(B)
San Andreas
Fault
San Francisco
Santa Cruz Basin
Salinas Basin
Santa Maria Basin
San Joaquin Basin
Bakersfield
Ventura Basin
Los Angeles
Los Angeles Basin
Pacific Ocean
0 80 160 km
Lost Hills
TEMBLOR
Belridge
Chico Martinez Creek
SAN ANDREAS FAULT
Buttonwillow
Railroad Gap
Bakersfield
Cymric
Elk Hills
Asphalto
S. Coles Levee
RANGE
Paloma
Buena Vista Hills
Midway Sunset
N
0 10 20 30 km

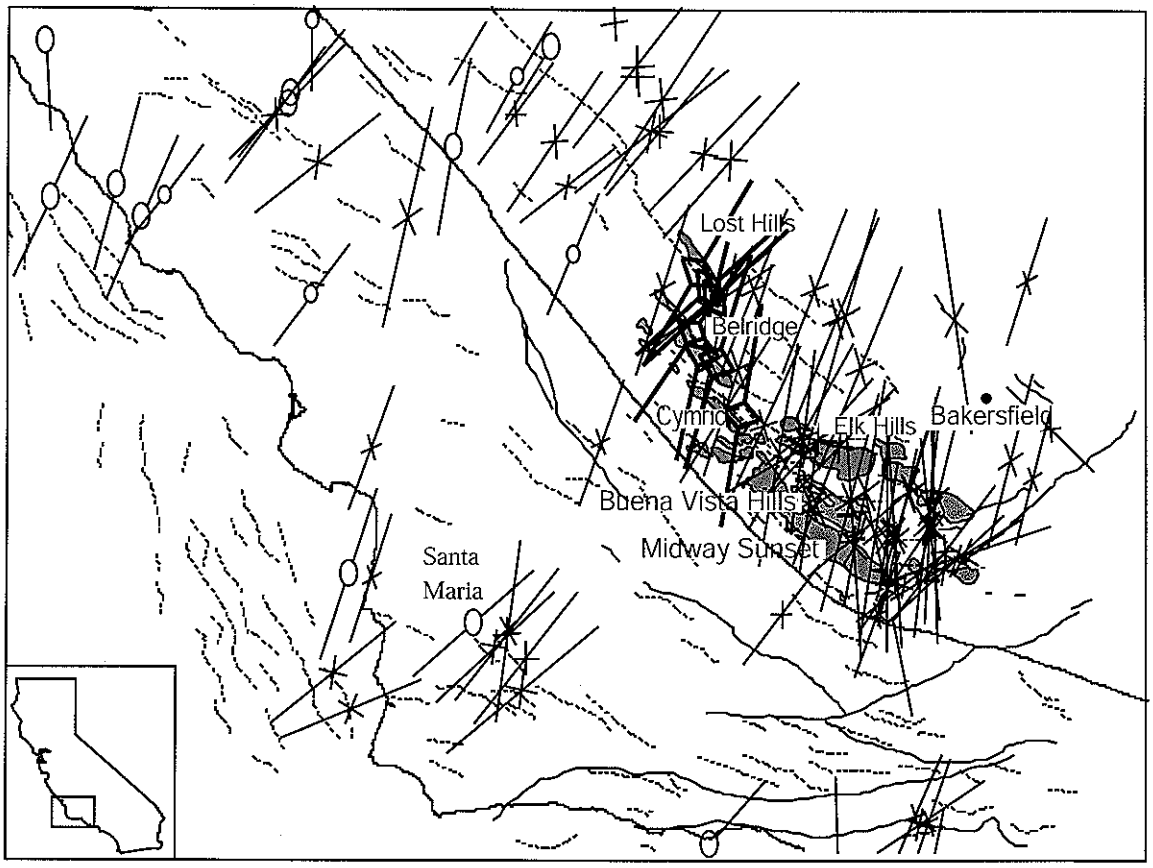

Earthquake Focal Mechanism

Well Bore Breakout

Hydraulic Fracture

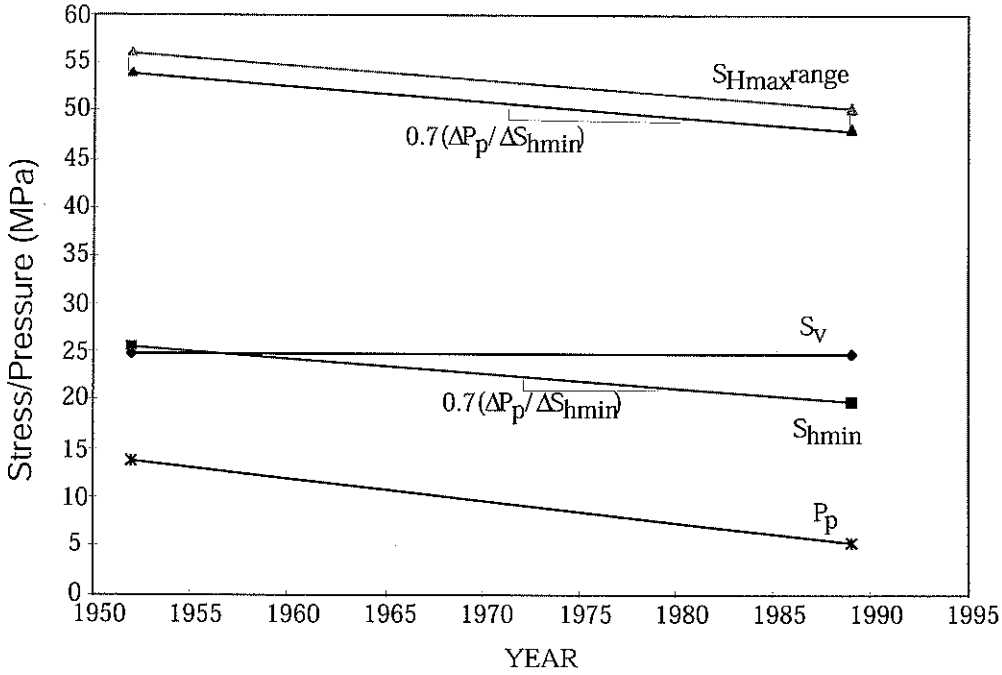
Stress/Pressure (MPa)
60
55
50
45
40
35
30
25
20
15
10
5
0
1950
1955
1960
1965
1970
1975
1980
1985
1990
1995
YEAR
S_{Hmax}range
0.7(ΔP_p/ΔS_{hmin})
S_v
0.7(ΔP_p/ΔS_{hmin})
S_{hmin}
P_p

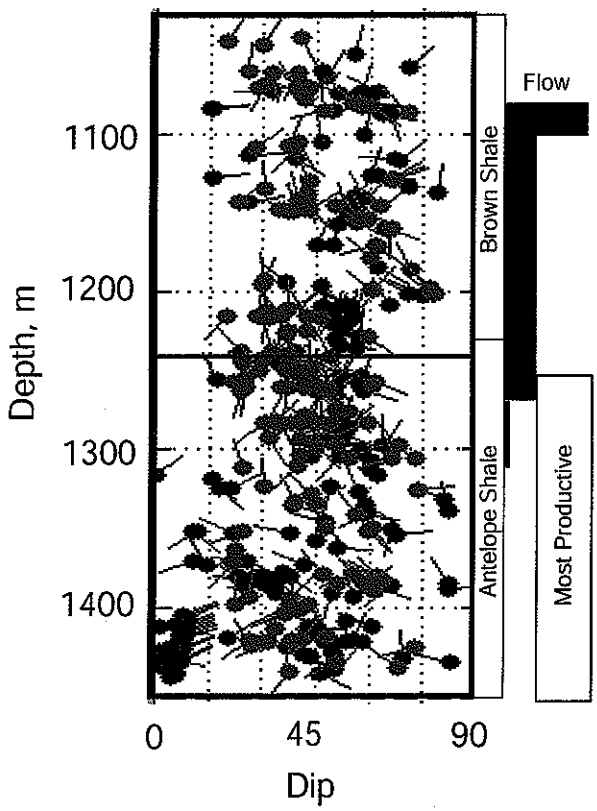
Flow
1100
1200
1300
1400
Depth, m
Brown Shale
Antelope Shale
Most Productive
0
45
90
Dip

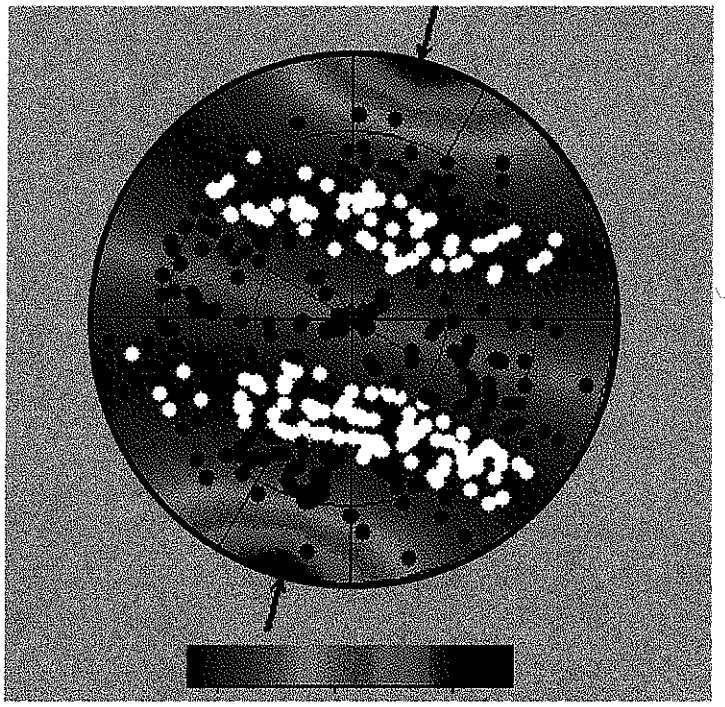
0
10
20
MPa

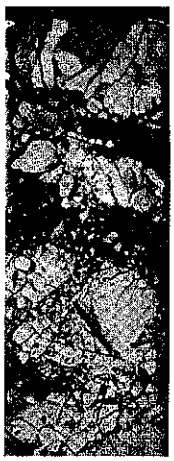

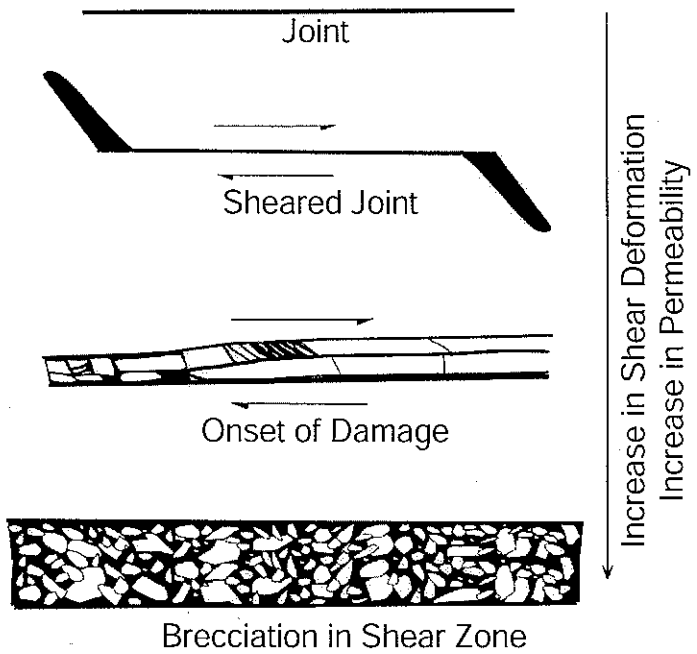
Joint
Sheared Joint
Onset of Damage
Brecciation in Shear Zone
Increase in Shear Deformation
Increase in Permeability